NeuroImage: Clinical 31 (2021) 102774

Contents lists available at ScienceDirect

NeuroImage: Clinical

journal homepage: www.elsevier.com/locate/ynicl

Fixel-based evidence of microstructural damage in crossing pathways improves language mapping in Post-stroke aphasia

Jie Zhang [a,b], Weihao Zheng [c], Desheng Shang [d], Yating Chen [b], Shuchang Zhong [b], Jing Ye [b], Lingling Li [a], Yamei Yu [e], Li Zhang [b], Ruidong Cheng [b], Fangping He [a], Dan Wu [f], Xiangming Ye [b], Benyan Luo [a,g,*]

[a] Department of Neurology & Brain Medical Center, The First Affiliated Hospital, Zhejiang University School of Medicine, Hangzhou, China
[b] Rehabilitation Medicine Center & Rehabilitation Research Institute of Zhejiang Province, Zhejiang Provincial People's Hospital, Affiliated People's Hospital, Hangzhou Medical College, Hangzhou, China
[c] School of Information Science and Engineering, Lanzhou University, Lanzhou, China
[d] Department of Radiology, The First Affiliated Hospital, Zhejiang University School of Medicine, Hangzhou, China
[e] Sir Run Run Shaw Hospital, School of Medicine, Zhejiang University, Hangzhou, China
[f] Key Laboratory for Biomedical Engineering of Ministry of Education, College of Biomedical Engineering and Instrument Science, Zhejiang University, Hangzhou, China
[g] Collaborative Innovation Center for Brain Science, Zhejiang University School of Medicine, China

ARTICLE INFO

Keywords:
Fixel-based analysis
Crossing fiber
Diffusion-weighted imaging
White matter
Aphasia
Stroke

ABSTRACT

Background: The complex crossing-fiber characteristics in the dual-stream system have been ignored by traditional diffusion tensor models regarding disconnections in post-stroke aphasia. It is valuable to identify microstructural damage of crossing-fiber pathways and reveal accurate fiber-specific language mapping in patients with aphasia.

Methods: This cross-sectional study collected magnetic resonance imaging data from 29 participants with post-stroke aphasia in the subacute stage and from 33 age- and sex-matched healthy controls. Fixel-based analysis was performed to examine microstructural fiber density (FD) and bundle cross-section alterations of specific fiber populations in crossing-fiber regions. Group comparisons were performed, and relationships with language scores were assessed.

Results: The aphasic group exhibited significant fixel-wise FD reductions in the dual-stream tracts, including the left inferior fronto-occipital fasciculus (IFOF), arcuate fasciculus, and superior longitudinal fasciculus (SLF) III (family-wise-error-corrected $p < 0.05$). Voxel- and fixel-wise comparisons revealed mismatched distributions in regions with crossing-fiber nexuses. Fixel-wise correlation analyses revealed significant associations between comprehension impairment and reduced FD in the temporal and frontal segments of the left IFOF, and also mapped naming ability to the IFOF. Average features along the whole course of dominant tracts assessed with tract-wise analyses attributed word-level comprehension to the IFOF ($r = 0.723$, $p < 0.001$) and revealed a trend-level correlation between sentence-level comprehension and FD of the SLF III ($r = 0.451$, $p = 0.021$). The mean FD of the uncinate fasciculus (UF) and IFOF correlated with total and picture naming scores, and the IFOF also correlated with responsive naming subdomains (Bonferroni corrected $p < 0.05$).

Conclusions: FD reductions of dual streams suggest that intra-axonal volume reduction constitutes the microstructural damage of white matter integrity in post-stroke aphasia. Fixel-based analysis provides a complementary method of language mapping that identifies fiber-specific tracts in the left hemisphere language network with greater specificity than voxel-based analysis. It precisely locates the precise segments of the IFOF for comprehension, yields fiber-specific evidence for the debated UF-naming association, and reveals dissociative subdomain associations with distinct tracts.

Abbreviations: AF, arcuate fasciculus; SLF, superior longitudinal fasciculus; IFOF, inferior fronto-occipital fasciculus; UF, uncinate fasciculus; FA, fractional anisotropy; DTI, diffusion tensor imaging; DWI, diffusion-weighted imaging; ILF, inferior longitudinal fasciculus; MdLF, middle longitudinal fasciculus; FOD, fiber orientation distribution; CSD, constrained spherical deconvolution; FBA, fixel-based analysis; FD, fiber density; FC, fiber-bundle cross-section; FDC, combined fiber density and bundle cross-section; TOI, tract of interest; VBA, voxel-based analysis; FWE, family-wise error; TPJ, temporoparietal junction.

* Corresponding author at: 79 Qingchun Road, Hangzhou 310003, China.
E-mail address: luobenyan@zju.edu.cn (B. Luo).

https://doi.org/10.1016/j.nicl.2021.102774
Received 6 March 2021; Received in revised form 16 July 2021; Accepted 22 July 2021
Available online 25 July 2021

1. Introduction

Ischemic stroke is the most common cause of acquired aphasia (Berthier, 2005). White matter impairment is involved in most cerebral infarction lesions, which is closely related to neurobehavioral and cognitive disability, including aphasia (Corbetta et al., 2015). Post-mortem research in patients with subcortical stroke lesions indicates demyelination and disruption of white matter architecture as chief hallmarks of white matter alterations after ischemic injury (Marin and Carmichael, 2019). White matter fibers have emerged as pivotal structures in the contemporary language model.

In the prevailing dual-stream language model, the dorsal and ventral tracts constitute two pathways between classical cortical language centers, which are essential for sound-to-articulation and sound-to-meaning mapping, respectively (Friederici, 2012; Hickok and Poeppel, 2007; Saur et al., 2008). To date, most diffusion imaging studies on post-stroke aphasia have used traditional tensor-derived metrics as reported by a recent review (Zhang et al., 2021). Their results constitute the fundamental of the current dual-stream language model. For instance, the left arcuate fasciculus (AF) and superior longitudinal fasciculus (SLF) play a speech production role (Han et al., 2016; Marchina et al., 2011; Pani et al., 2016), while the function of the left inferior fronto-occipital fasciculus (IFOF) in semantic processing has been well-established in numerous studies (Han et al., 2013; Harvey and Schnur, 2015; Harvey et al., 2013; Ivanova et al., 2016; Xing et al., 2017; Zhang et al., 2018). However, the tract-linguistic correlates of specific tracts such as the uncinate fasciculus (UF) are still disputed (Catani et al., 2013; Ivanova et al., 2016). For these previous diffusion tensor imaging (DTI) studies, the historical inconsistencies and inaccuracy of anatomical-functional mapping might be attributed to the poor biological plausibility and interpretability of the tensor model. The prevailing voxel-wise metric fractional anisotropy (FA) cannot reflect the fiber-specific white matter characteristics in regions containing crossing fibers.

With diffusion-weighted imaging (DWI) developments, advanced evidence has demonstrated that most white matter voxels contain crossing-fiber populations, especially in the language pathways (Jeurissen et al., 2013; Raffelt et al., 2015). In the dorsal stream of language pathways, the AF is characterized by a large proportion of crossing fibers with high posterior curvature (Raffelt et al., 2015). The SLF traverses the centrum semiovale along with the corpus callosum and corticospinal tract (Jeurissen et al., 2013; Mito et al., 2018). Regarding the ventral stream, the IFOF, inferior longitudinal fasciculus (ILF), and middle longitudinal fasciculus (MdLF) run close together (Catani et al., 2002; Duffau et al., 2013). For the UF, its posterior portion crosses the ILF (Hau et al., 2017). The crossing-fiber problem of complex fiber tracts in above language pathways poses a challenge to aphasia researchers.

To overcome the limitations of tensor-derived metrics, advanced diffusion models have been developed to obtain fiber orientation distributions (FODs). Constrained spherical deconvolution (CSD) is one of the most robust methods for FOD estimation (Tournier et al., 2007). Based on CSD, fixel-based analysis (FBA) is utilized to extract metrics for specific fiber populations within each voxel, defined as fixels (Raffelt et al., 2017; Tournier et al., 2007). This approach introduces fixel-wise metrics to investigate crossing fibers within voxels, including fiber density (FD), fiber-bundle cross-section (FC), and the combined fiber density and bundle cross-section (FDC).

FD measures the intra-axonal volume of axons in each voxel compartment, capturing microstructural information of a specific fiber population including the within-voxel number of axons and axon volume (Raffelt et al., 2017). FC measures the cross-sectional size of fiber bundles as an index of macroscopic morphology. As a combined measure accounting for both macroscopic and microscopic feature, FDC is reflective of the total capacity to relay information (Raffelt et al., 2017). Voxel-wise fiber-specific metrics, including complexity, can be derived from the FD, thereby providing detailed within-voxel features (Riffert et al., 2014). Combining fixel-wise and fixel-derived metrics could help to improve the delineation of comprehensive pathological white-matter characteristics.

FBA studies have hitherto focused on neurodegenerative diseases (Mito et al., 2018; Rau et al., 2019; Zarkali et al., 2020), preterm brain development (Pannek et al., 2018; Pecheva et al., 2019), and traumatic brain injury (Verhelst et al., 2019; Wallace et al., 2020). Cerebrovascular diseases have received scant attention. One study on ischemic stroke at the subacute stage reported that reduced FD and FC were not confined to lesion-adjacent areas but extended beyond connected tracts (Egorova et al., 2020). Previous research enrolled post-stroke aphasia patients at the early stage to reduce the influence of heterogeneity from clinical profiles and white matter integrity (Yang et al., 2017). Our study also focused on the subacute stage, considering it is a critical time for neural plasticity (Bernhardt et al., 2017), and should be a target time course for identifying predictive biomarkers or disease progress (Egorova et al., 2020). The relationship between fiber-specific white matter alterations and advanced dysfunction after ischemic stroke remains unclear, particularly in terms of language impairment.

In the first FBA study of post-stroke aphasia, we aimed to disentangle crossing-fiber pathways and to investigate the fiber-specific language associations in the dual-stream pathways. We hypothesized that fiber-specific microstructural characteristics could lead to more precise mapping of language subdomains in post-stroke aphasia.

2. Methods and materials

2.1. Participants

The patients in this study were recruited prospectively from the Department of Neurology and Brain Medical Center of the First Affiliated Hospital of Zhejiang University School of Medicine between October 2018 and December 2020. Eligibility criteria included a history of initial left-hemisphere ischemic stroke during the early subacute stage (7 days to 1 month), aphasia confirmed by the language scale, age 18–80 years, right-handedness, Chinese as a first language, and education experience $\geq$ 6 years. Subjects were excluded if they had pre-existing neurological or psychiatric disorders, a history of psychoactive medication or of alcohol use disorder, or magnetic resonance imaging contraindications. Age-, sex-, and education-matched healthy volunteer controls were also recruited via local advertisements. We chose subacute stroke patients to moderate the impact of cerebral edema on diffusion imaging in the early stage and to avoid the confounding effect of white matter alterations secondary to cortical lesions (e.g., Wallerian degeneration), and thus focused on the direct ischemic damage to the white matter. We initially recruited 32 patients and 34 controls. Three patients with poor imaging quality were excluded, while the magnetic resonance imaging data of one healthy control were unavailable due to incomplete volumes of the DWI sequence. The final cohort consisted of 62 participants (29 patients, 33 healthy controls). All participants provided written informed consent in accordance with the tenets of the Declaration of Helsinki. The study protocol and consent form were approved by the Local Research Ethics Committee of the First Affiliated Hospital, Zhejiang University School of Medicine.

2.2. Language assessment

The Aphasia Battery of Chinese was used to assess language performance at the time of aphasia onset (Gao, 2006). The assessment was conducted by a certified examiner (J.Y.), and the scores were checked and documented by another blinded researcher (Y.Y.). Language domains included spontaneous speech, repetition, comprehension, naming, reading, writing performance, and overall aphasia severity, as measured by the aphasia quotient. Subdomains of comprehension (word- and sentence-level comprehension) and naming (picture, color, and responsive naming) were also investigated.

2.3. Image acquisition

Magnetic resonance imaging data were acquired using a 3-T Signa HDxt 2.0 scanner (GE Healthcare, Chicago, IL). DWI was performed using a spin-echo, single-shot, echo-planar imaging sequence with the following parameters: 40 non-collinear diffusion-weighted directions (b = 2000 s/mm^2) and 3 interspersed b0 volumes; field of view = 256 mm × 256 mm; acquisition matrix = 128 × 128; voxel size = 2 × 2 × 3 mm; repetition time = 5100 ms; echo time = 66.2 ms; 50 slices with no gap. Structural T1-weighted imaging was performed using a high-resolution, three-dimensional brain volume imaging sequence (voxel size = 1 × 0.5 × 0.5 mm; repetition time = 7.8 ms; echo time = 3.0 ms; flip angle = 7°).

2.4. Image pre-processing

2.4.1. Structural image processing

The T1-weighted images were utilized to delineate ischemic lesions. The lesion masks were drawn manually using ITK-SNAP by two experienced neurological researchers (J.Z. and S.Z.). All subject binary lesion masks were normalized into the standard space (MNI152 template). The map in Fig. 1. shows the distribution of lesion coverage. The Tissue Volume module was used to compute the intra-cranial volume based on segmented T1-weighted data using the Computational Anatomy Toolbox 12 in SPM12 (https://www.fil.ion.ucl.ac.uk/spm/software/spm12).

2.4.2. DWI pre-processing and CSD modelling

The DWI data were processed using a single-tissue CSD pipeline (Tournier et al., 2007) that included multiple pre-processing steps in MRtrix3 (v3.0.0) (www.mrtrix.org) (Tournier et al., 2019). The standardized steps included estimating the DWI noise level, denoising based on random matrix theory, eddy current-induced distortion correction and within-volume motion correction using scripts that interfaced with the FMRIB Software Library (v6.0.2) (Andersson et al., 2017; Andersson et al., 2016; Andersson and Sotiropoulos, 2016), bias field correction using Advanced Normalization Tools (Avants et al., 2011), global intensity normalization, and upsampling to an isotropic voxel size of 1.3 mm. Single-shell response functions were computed to represent single-fiber white matter, and a group-averaged response function was obtained to perform CSD of all subjects. The T1 lesion masks in the structural space were linked to the diffusion space using FLIRT (FMRIB's Linear Image Registration Tool) (Greve and Fischl, 2009). Voxels of lesioned areas were prevented from driving the registration process as well as contributing to the resulting template. Lesioned areas of subjects were excluded from aggregation, and an unbiased study-specific FOD template including data of all subjects was then created. All subject FOD images were registered to the FOD template and warped into the common template space after masking lesioned tissue.

2.5. Multi-level analytic strategies

Multi-level analytic strategies and metrics are summarized in Fig. 2 and are clarified as follows.

2.5.1. Fixel-wise metrics

To estimate the orientation and number of fixels in each voxel, each FOD lobe was segmented; the apparent density value per fixel was then obtained. The fixels in the template space were then reoriented in accordance with the local transformation of the warps. The subject fixel in the matching voxel was identified for each template fixel, and the FD value of this corresponding subject fixel was assigned to that template fixel. FD, FC, and FDC were then obtained to detect fiber-specific white matter pathologies in crossing-fiber regions with greater sensitivity and interpretability than tensor-derived metrics (Raffelt et al., 2017).

2.5.2. Voxel-wise metrics

Two categories of voxel-wise metrics were calculated to depict detailed microstructure (see Supplemental Method 1). Fixel-derived voxel-wise metrics included FDi and complexity. FDi is defined as the FD of the ith largest peak of the fiber orientation density function within a voxel (Riffert et al., 2014). FD1, FD2, and FD3 measure the density of the primary, secondary, and tertiary fiber populations, respectively, while complexity compares relative density differences of distinct fiber populations within a voxel. Tensor models were estimated to obtain

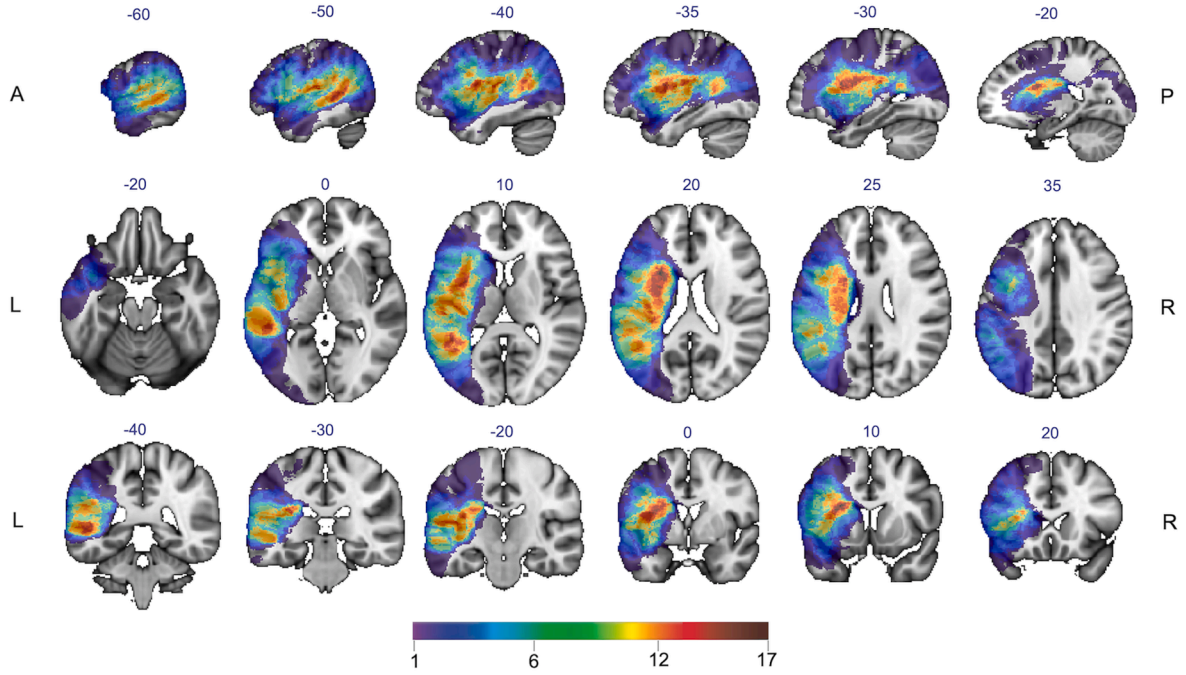

Fig. 1. Lesion overlay of all participants with post-stroke aphasia. The colors indicate the number of patients with lesions at each voxel, with warmer colors indicating a greater extent of lesion overlap (the color bar ranges from 1 in purple to 17 in dark red). (For interpretation of the references to color in this figure legend, the reader is referred to the web version of this article.)

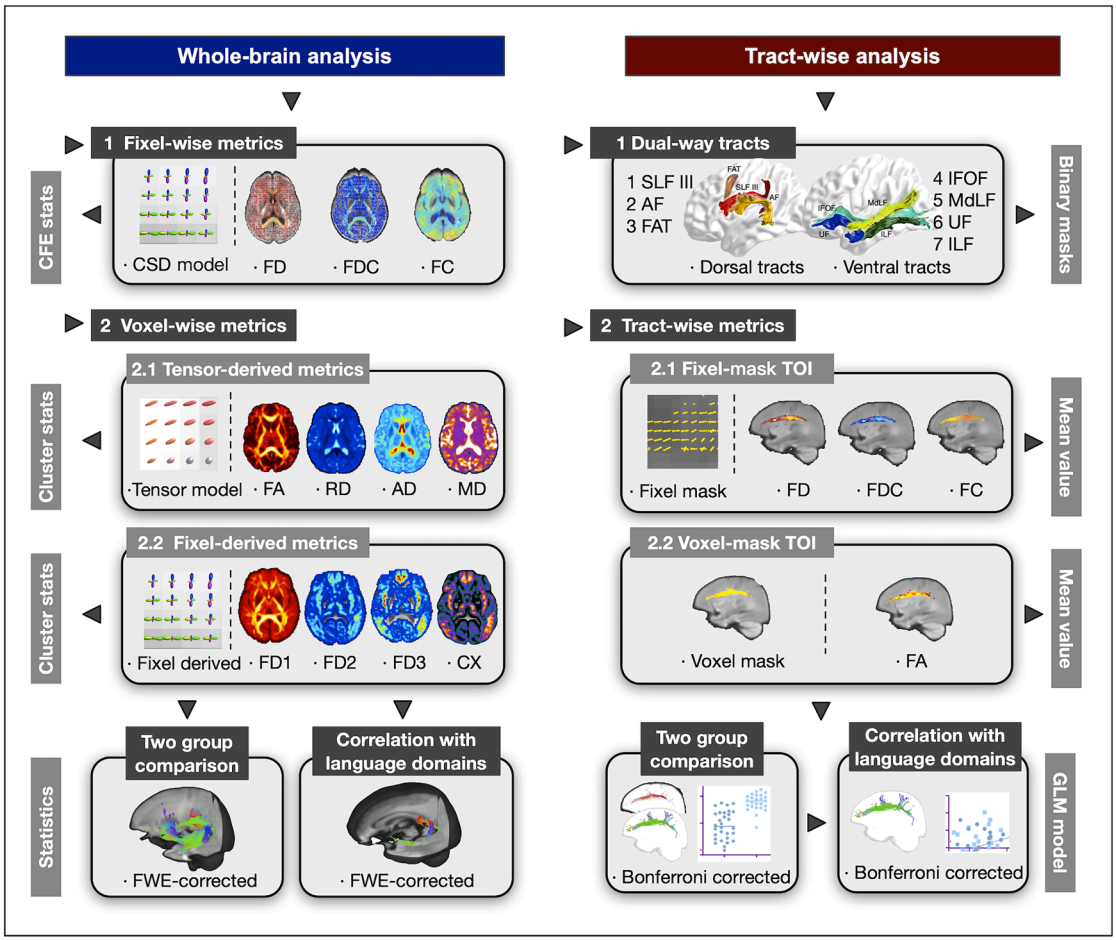

Fig. 2. Multi-level analytic strategies and metrics for diffusion images. The strategies of this study include whole-brain analysis and tract-wise analysis, and each analysis strategy uses fixel-wise and voxel-wise metrics. AD = axial diffusivity; AF = arcuate fasciculus; CX = complexity; CSD = constrained spherical deconvolution; FA = fractional anisotropy; FC = fiber cross-section; FD = fiber density; FDC = fiber density and cross-section; FWE = family-wise error; IFOF = inferior fronto-occipital fasciculus; ILF = inferior longitudinal fasciculus; MD = mean diffusivity; MdLF = middle longitudinal fasciculus; RD = radial diffusivity; SLF = superior longitudinal fasciculus; TOI = tract of interest; UF = uncinate fasciculus.

voxel-wise FA, axial diffusivity, radial diffusivity, and mean diffusivity. Gaussian smoothing was applied to voxel-wise images explicitly with a specified full-width at a half maximum of 3 mm.

FBA and voxel-based analysis (VBA) results were respectively thresholded to produce the significant fixels and clusters. The significant fixels of FBA and clusters of VBA results were binarized into fixel- and voxel-wise masks. Fixel-wise masks were then transformed into voxel level using the *fixel2voxel* command for further calculation between images. FBA-VBA overlap and mismatch were respectively located by multiplication and subtraction operations between FBA-VBA result masks. For better visualization, the spatial correspondence was compared by rendering FBA and VBA results in the same three-dimensional space.

2.5.3. Tract-wise metrics

Given that most tracts in the language network consist of long-range fibers, atlas-based tract-wise metrics were extracted to measure the average features along the whole course of specific tracts of interest (TOIs) and complement whole-brain analyses. CSD-derived whole-brain probabilistic tractography was performed to obtain whole-brain template tractogram based on the data from the current study. Streamlines were seeded at random, and 20 million streamlines were selected. The cut-off value of FOD amplitude for terminating tracks was 0.10, and the maximum angle between successive steps was 22.5°. Spherical-deconvolution informed filtering of tractograms was then used until 2 million streamlines remained (Smith et al., 2013). We chose seven dual-stream tracts (the SLF III, AF, IFOF, UF, ILF, MdLF, and frontal aslant tract) as TOIs defined by XTRACT, a novel automated tractography protocol (see detailed techniques in Supplemental Method 2) (Warrington et al., 2020). Fixel masks of TOIs aimed to identify more specific changes in tract-wise metrics in crossing-fiber regions than traditional voxel masks. For complementary information, we also extracted average tensor-derived metric FA from voxel masks of TOIs for between-group comparisons. We performed tract-wise correlation analyses for TOI metrics of significant between-group differences.

2.6. Statistical analysis

For whole-brain FBA, connectivity-based fixel enhancement was applied to conduct tract-specific smoothing and to enhance the statistical map (Raffelt et al., 2015). For whole-brain VBA, threshold-free cluster enhancement was used to produce the statistical map using the *mrclusterstats* command in MRtrix3 (v3.0.0). Family-wise error (FWE) correction was performed for whole-brain analyses using non-parametric bootstrapping (5000 permutations). The general linear models (GLMs), two-group difference adjusted for nuisance covariate and single-group correlation with additional covariate, were used for tests in whole-brain analyses. Statistical significance was set at FWE-corrected $p < 0.05$.

For tract-wise analyses, within-TOI mean values were compared

between patients and controls using GLMs in IBM SPSS Statistics for macOS (v25; IBM, Armonk, NY). Considering the language scores were not normal distribution, Spearman's partial correlation analysis was used to investigate the relationship between language scores and within-TOI mean values in the stroke group. The significance threshold was adjusted by the Bonferroni correction ($p < 0.05/k$, k = number of multiple comparisons including selected tracts and evaluated metrics, see details in Supplemental Method 2).

Age, sex, education level, whole-brain averaged values, lesion volume, and cortical involvement of lesion were considered as nuisance covariates for the results. Motor dysfunction level was also included for further sensitivity analysis. Intracranial volume was an added moderator of FC and FDC to exclude the influence of head size.

3. Results

3.1. Demographic characteristics and behavioral findings

A total of 29 patients (59.2 ± 12.3 years, 21 males) with post-stroke aphasia and 33 healthy volunteers (54.6 ± 13.1 years, 19 males) were recruited. The mean time from stroke onset to enrollment was 13.2 (7.3) days. No significant between-group differences in age, sex, education level, or intracranial volume were observed (Table 1). Diverse behavioral profiles of aphasia were collected (Supplemental Table 1).

3.2. Whole-brain FBA

3.2.1. Group-wise comparisons

Whole-brain FBA revealed reduced FD in aphasia patients compared to the controls. As shown in Fig. 3A, most regions with fixels showing significant FD reductions were located within dual-stream tracts (the left SLF III, AF, IFOF, MdLF, and ILF), as well as the left anterior thalamic radiation, splenium, and radiations of the corpus callosum (FWE-corrected $p < 0.05$). By adding motor dysfunction level as a covariate, the sensitivity analysis showed that reduced FD was mainly confined to dual-stream tracts (Supplemental Fig. 1). The greatest FD reductions occurred in the temporal stem and frontal segments of the left IFOF (Fig. 3A, right panel). The FDC reduction showed a similar but smaller distribution confined to the left ventral tracts (IFOF and ILF), the anterior thalamic radiation, and corticospinal tract. Only the corticospinal tract exhibited FC reductions and almost no FC changes after the sensitivity analysis introducing the motor covariate (Supplemental Fig. 1). Fig. 3B showed zoomed fixels of significant fiber-specific populations in crossing-fiber regions.

Table 1
Demographic characteristics and medical information of participants (n = 62).

	Aphasia Patients n = 29	Healthy Controls n = 33	Statistic
Sex, male (%)	21 (72.4)	19 (57.6)	$\chi^2(1) = 1.484$, P = 0.223
Age, years (SD)	59.2 (12.3)	54.6 (13.1)	t(60) = 1.442, P = 0.155
Education, years (SD)	10.0 (3.7)	10.4 (4.2)	Z = -0.512*, P = 0.609
Time post-stroke, days (SD)	13.2 (7.3)	–	–
Handedness, right (%)	29 (100)	33 (100)	–
ICV, cm^3 (SD)	1549.5 (155.0)	1482.2 (136.2)	t(60) = 1.822, P = 0.073
Lesion volume, mL (SD)	52.7 (48.8)	–	–
Cortical involvement of lesion, % (SD)	53.8 (26.4)	–	–

Notes: Data are shown as mean (SD) or number (%). Reported P-values from two-sample independent *t*-test for age and intracranial volume, Mann-Whitney *U* test for the non-normal variable education year, and chi-squared test for male proportion and handedness. ICV = intracranial volume; SD = standard deviation. *: Z value was reported for Mann-Whitney *U* test.

3.2.2. Fixel-language mapping

Fig. 4A shows a positive correlation between the total comprehension score and fixel-wise FD in the left IFOF and tapetum of the corpus callosum of patients with aphasia (FWE-corrected $p < 0.05$). The IFOF segment around the limen insulae showed the greatest correlation. A positive correlation with word-level comprehension was also found in the left IFOF and the corpus callosum, with a greatest correlation in the frontal segment of the IFOF. The total naming score positively correlated with FD in the left IFOF (Fig. 4B). The significant correlation between FD and picture naming was located at the temporal segment of the left IFOF, while color naming was mapped to the left IFOF and tapetum of the corpus callosum. Positive associations between responsive naming and FD were also concentrated at the temporal segment of the left IFOF segment and tapetum of the corpus callosum. No correlations with FC or FDC were found.

3.2.3. Whole-brain VBA-FBA mismatch

Detailed whole-brain VBA results are shown in Supplemental Fig. 2. As shown in Fig. 5, some significant clusters of VBA and FBA results overlapped, including the centrum semiovale through which the left SLF III and AF pass. In the centrum semiovale, reduced FD, FA, and axial diffusivity, as well as increased radial diffusivity, FD3, and complexity were observed (Fig. 5, blue rectangle). We found mismatched regions in terms of positive spatial distributions. The voxels in the left temporoparietal junction (TPJ) showed reductions in FA, while the corresponding regions exhibited no significant fixel-wise alterations (Fig. 5, red rectangle). There was also decreased axial diffusivity and increased complexity and FD3 in the left TPJ (Supplemental Fig. 2). Zoomed FOD models showed that the TPJ contained crossing-fiber populations, including the dorsal tract intersecting with the ventral tract and the radiation of the corpus callosum.

3.3. Tract-wise analysis

3.3.1. Group-wise comparisons

Tract-wise analyses of left dual streams revealed reduced mean FDs within the fixel masks of the AF ($F = 12.18$, $p = 0.001$), IFOF ($F = 19.29$, $p < 0.001$), and UF ($F = 10.56$, $p = 0.002$) in post-stroke aphasia (Fig. 6). Of these, the IFOF had the highest reduction percentage (17.77%, 95% CI 10.48–25.05%). Only the IFOF exhibited significant FDC decrease ($F = 15.16$, $p < 0.001$). No group difference of tract-wise FC was reported. Regarding tensor-derived FA, we observed extensive reductions in AF ($F = 52.40$, $p < 0.001$), SLF III ($F = 30.30$, $p < 0.001$), IFOF ($F = 28.80$, $p < 0.001$), and MdLF ($F = 30.72$, $p < 0.001$).

3.3.2. Tract-wise language correlations

The tract-wise mean FD exhibited significantly positive correlations with comprehension and naming domains (Fig. 7). The left IFOF ($r = 0.646$, $p = 0.002$) and SLF III ($r = 0.524$, $p = 0.006$) showed correlations with the total comprehension score (Fig. 7A). Word-level comprehension subdomain significantly correlated with the IFOF ($r = 0.723$, $p < 0.001$), while sentence-level comprehension subdomain showed a trend-level positive correlation with the SLF III ($r = 0.451$, $p = 0.021$). No significant correlation between the mean FD of left UF and comprehension domain was reported. Regarding naming domain, we found that the mean FDs of the left IFOF and UF were significantly associated with the total naming score (IFOF: $r = 0.671$, $p < 0.001$; UF: $r = 0.651$, $p = 0.001$) and picture naming subdomain (IFOF: $r = 0.656$, $p = 0.001$; UF: $r = 0.646$, $p = 0.001$; Fig. 7B). In addition, the mean FD of the IFOF was also correlated with responsive naming subdomain ($r = 0.600$, $p = 0.002$), and exhibited trend-level positive correlation with a color naming ($r = 0.542$, $p = 0.007$). Compared to the mean FD, the significant correlations with tract-wise mean FA of the left IFOF were found within naming domain (total naming score: $r = 0.680$, $p < 0.001$; picture

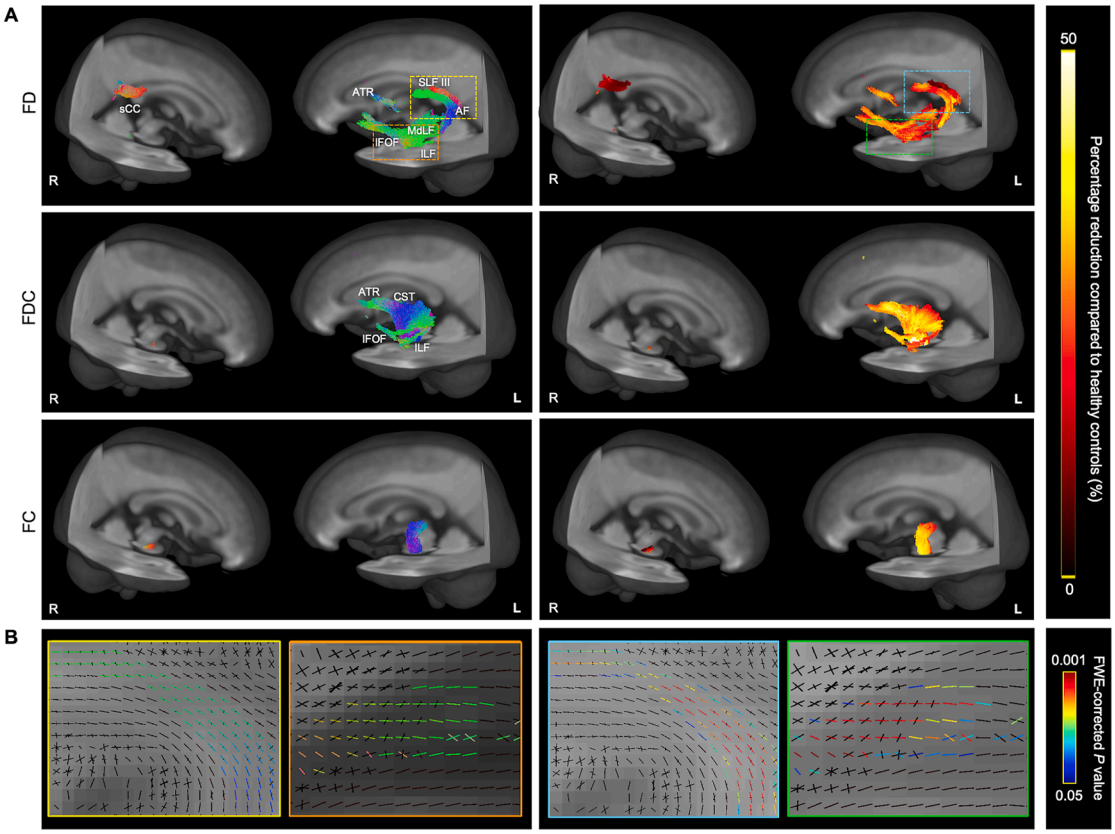

Fig. 3. Significant fiber-specific reductions of whole-brain fixel-wise metrics in post-stroke aphasia compared to controls. A, Tract-specific streamlines represent mapped fixels with significantly reduced fiber density (FD), fiber density and bundle cross-section (FDC), and fiber-bundle cross-section (FC) values on the population-template, displayed as three-dimensional streamlines cropped from the template tractogram at FWE-corrected $P < 0.05$. B, Enlarged crossing-fiber areas with significant fixels of FD reductions. Left panels: colors are encoded by fixel direction (green: anterior-posterior, blue: superior-inferior, red: left–right); right panels: streamline points are colored by percentage reductions, and zoomed fixels are colored by FWE-corrected P-values. ATR = anterior thalamic radiation; CST = corticospinal tract; sCC = splenium of the corpus callosum; Tap = tapetum of the corpus callosum. (For interpretation of the references to color in this figure legend, the reader is referred to the web version of this article.)

naming subdomain: $r = 0.673$, $p < 0.001$), and only a trend-level correlation was reported with word-level comprehension ($r = 0.540$, $p = 0.007$). No significant correlation was found with mean FA of left SLF III, AF, and MdLF.

4. Discussion

This study reports a reduced microstructural FD of fixels and reduced tract-wise mean FD in the left SLF III, AF, and IFOF, indicating consistent convincing evidence of extensive intra-axonal volume reduction of axons in the dual-stream pathways of aphasic patients. We found that the fixel-wise FD in the left IFOF was associated with comprehension and naming. Tract-wise analyses revealed dissociative associations with language subdomains, attributing word-level comprehension to the IFOF and sentence-level comprehension to the SLF III. Our analyses also yielded more fiber-specific evidence regarding the debate of the UF-naming association. Comparing with conventional voxel-wise results, FBA showed the advantages of greater specificity in mapping injured fibers, and could locate more precise segments along the long-range tracts.

4.1. Altered dual-stream microstructure in post-stroke aphasia

Considering that this study focused on subacute stroke within 4 weeks of the stroke event, the white matter impairment was mostly caused by direct subcortical damage rather than long-term injury secondary to cortical lesions. The locations of extensive FD reduction (i.e., dual-stream pathways) agreed with the findings of previous tensor-derived diffusion studies in aphasic patients: the dorsal stream SLF (Han et al., 2016; Ivanova et al., 2016; Yang et al., 2017) and AF (Kim and Jang, 2013; Marchina et al., 2011; Y. Zhang et al., 2010) and the ventral stream dominated by the left IFOF (Han et al., 2013; Harvey and Schnur, 2015; Harvey et al., 2013; Xing et al., 2017; Zhang et al., 2018) were the most commonly affected. However, the high percentage of crossing fibers in the language pathways is a critical issue that must be considered. Although previous studies reported changes at the tract-wise level, the mean FA of tracts is inaccurate because tensor-derived tractography is not fiber-specific. Moreover, the biological plausibility and interpretability of FA is poor because reduced FA can be caused by multiple potential microstructural tissue characteristics including decreased myelination, reduced axon density, and poor axon coherence (Johansenberg and Behrens, 2013).

The FBA approach not only locates the accurate segment of fiber-specific tracts but also attributes impaired white matter integrity to microstructural intra-axonal volume reduction. Extensively reduced FD suggests microstructural intra-axonal volume reduction of specific fiber populations (e.g., axonal loss) as the pathological substrate of subacute post-stroke aphasia. The absence of FC alterations indicates that macroscopic cross-sectional change of fiber bundles is not obvious in the subacute stage of stroke. As evidence indicates that dissociable FBA metrics results from a stroke, fiber density reductions could precede macroscopic fiber cross-section changes during different stages of neurodegeneration (Egorova et al., 2020).

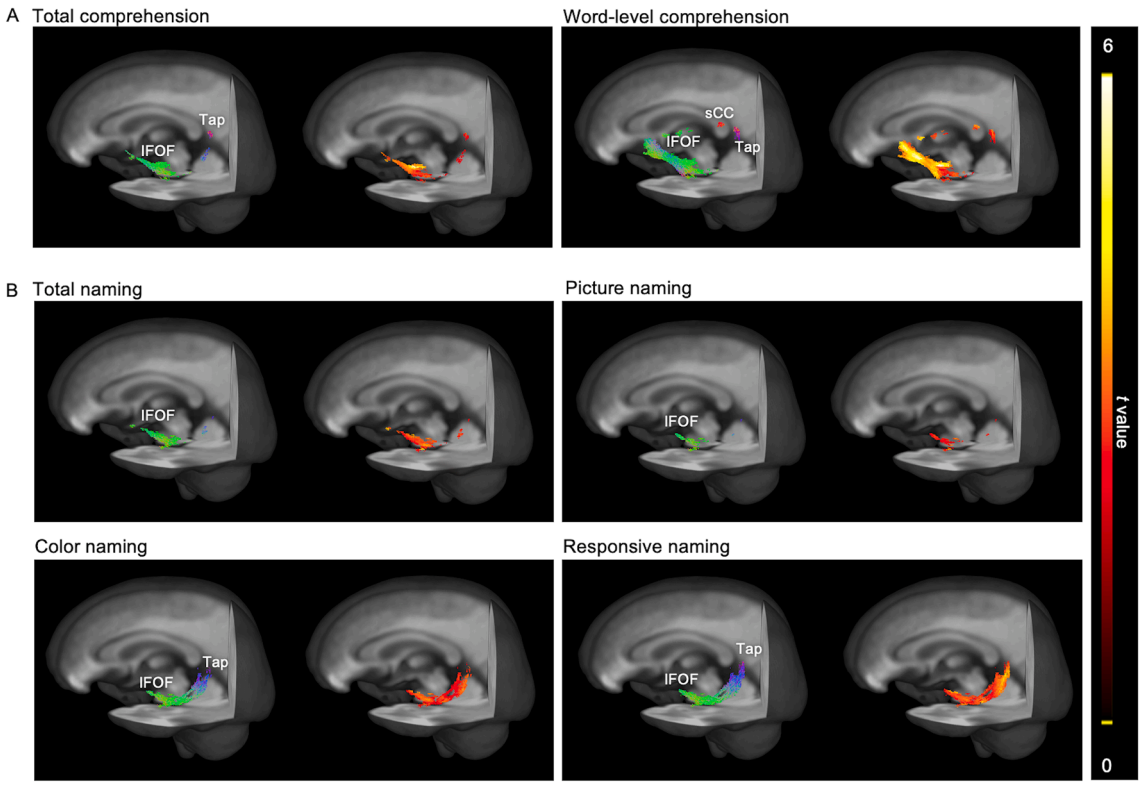

Fig. 4. Whole-brain correlation mapping between language domains and fixel-wise fiber density (FD) in post-stroke aphasia. Streamlines are cropped from the template tractogram to show significant fixels at family-wise error-corrected $P < 0.05$. A, Positive correlations between comprehension domain and FD. B, Positive correlations between naming domain and FD. Left panels: colors are encoded by fixel direction (green: anterior-posterior, blue: superior-inferior, red: left–right); right panels: streamline points are colored by t values of correlation analyses. sCC = splenium of the corpus callosum; Tap = tapetum of the corpus callosum. (For interpretation of the references to color in this figure legend, the reader is referred to the web version of this article.)

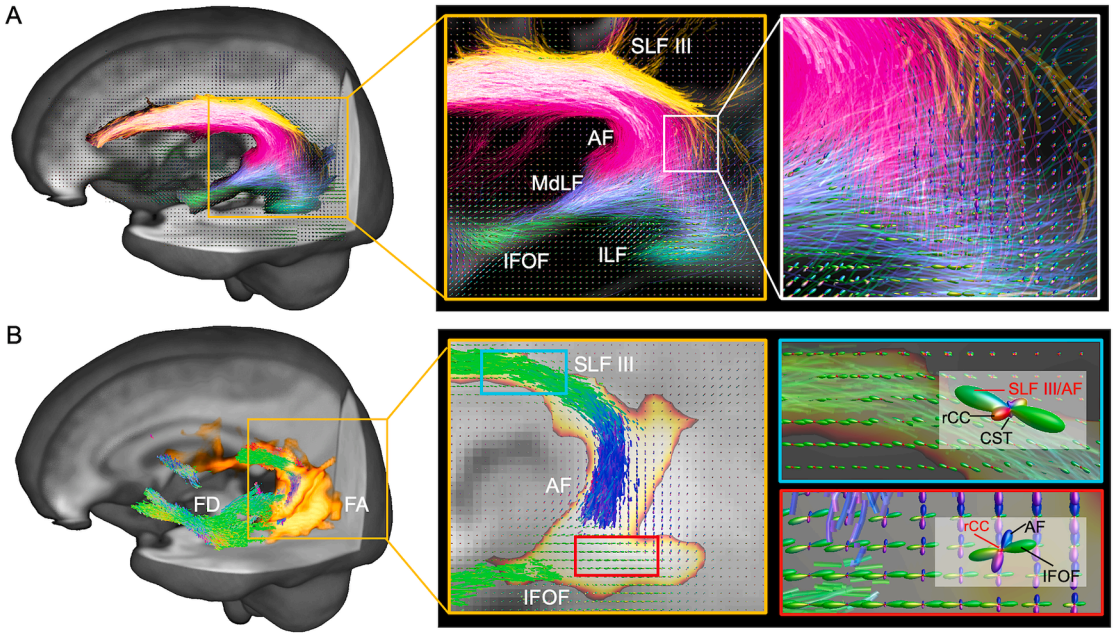

Fig. 5. Spatial distribution comparison of between fixel- and voxel-wise metrics results with zoomed fiber orientation distributions (FODs) in post-stroke aphasia compared to controls. A, Spatial correspondence of dual-way tracts in the vicinity of the significant results. The zoomed rectangles show the regional crossing-fiber nexuses of the left major tracts (magenta: AF, green: IFOF, turquoise: ILF, blue: MdLF, yellow: SLF III). B, Significant fixels of reduced fiber density (FD) (three-dimensional streamlines colored by fixel direction, mainly in green and blue), and significant clusters of reduced fractional anisotropy (FA) (three-dimensional streamlines colored in yellow). Zoomed rectangles exhibit regional crossing-fiber orientations within corresponding voxels (overlapped region in blue rectangle: centrum semiovale; mismatched region in red rectangle: temporoparietal junction). CST = corticospinal tract; rCC = radiation of the corpus callosum. (For interpretation of the references to color in this figure legend, the reader is referred to the web version of this article.)

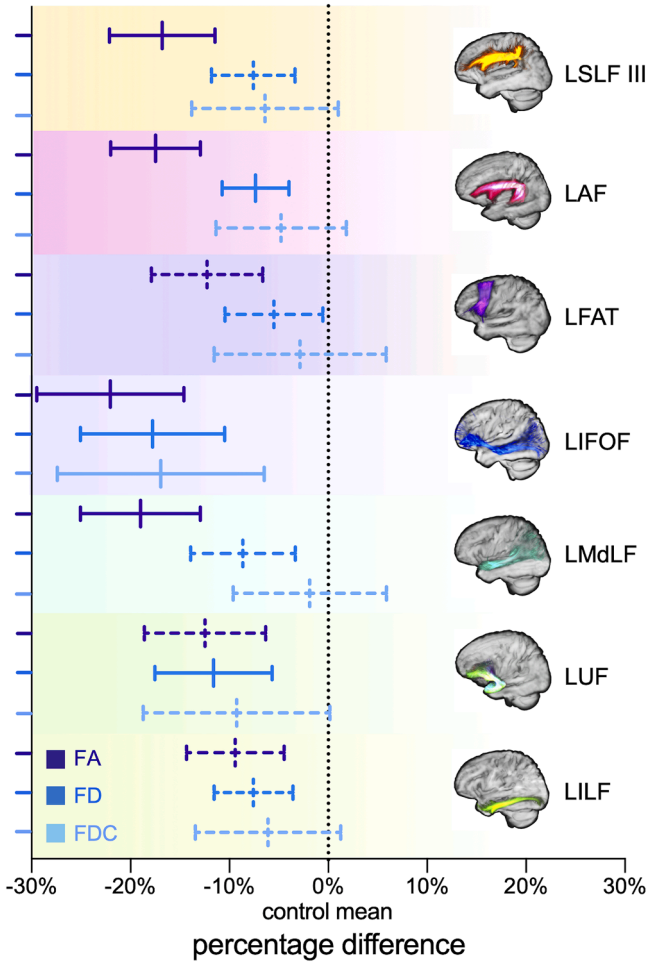

Fig. 6. Percentage differences of mean diffusion metrics within left tracts of interest compared to controls. Solid lines indicate significant reduced mean metrics of a specific tract (Bonferroni corrected $p < 0.05$). FA = fractional anisotropy; FD = fiber density; FDC = fiber density and bundle cross-section.

4.2. Typical crossing-fiber regions with VBA-FBA mismatch

To investigate the regional crossing-fiber configurations, we compared the spatial patterns of significant clusters between VBA and FBA. We also noted mismatched regions, such as the vicinity of left TPJ. The mismatch showed significant VBA metric alterations with negative FBA changes in the TPJ. Representative FOD patterns might account for differences in local fiber populations. The TPJ belongs to the Geschwind territory involved in phonological repetition (Forkel et al., 2020; Fridriksson et al., 2010) and high-level language processing (Carotenuto et al., 2018). The TPJ may contain distinct cell populations and complex crossing-fiber populations at the nexus of multiple processing streams, thereby playing a broad integrative role (Carter and Huettel, 2013). Therefore, it was difficult to identify the affected fiber bundle based on the reduced FA of the voxels in the TPJ. Complexity is mostly inversely proportional to FA, and higher complexity values in the TPJ of aphasic patients appear to be caused by reduced density of primary fiber populations or increased density of non-primary fiber populations (Grazioplene et al., 2018). In our study, the higher density of the tertiary fiber population (i.e., radiation of the corpus callosum) was observed in the left TPJ, suggesting potentially increased connectivity between bilateral hemispheres. Recruitment of the right homologues after a left-hemispheric stroke, as well as the association between language and between-hemisphere connectivity of the corpus callosum, have been previously observed (Crinion and Price, 2005; Kyeong et al., 2019). Future longitudinal studies might reveal dynamic changes of language specific fibers, and verify the prognosis of between-hemisphere connectivity over time after the degeneration of primary pathways.

4.3. Language mapping with improved locations and dissociable subdomains

Most of the present correlation results are in line with the documented relationship between dual-stream tracts and language. Numerous studies have demonstrated the semantic role of the left IFOF (Han et al., 2013; Ivanova et al., 2016; Xing et al., 2017; Zhang et al., 2018), as well as the association between the left AF and repetition ability involved in sound-to-motor mapping (Forkel et al., 2014; Marchina et al., 2011; Zhang et al., 2010). However, compared to the voxel-wise results, the FBA results provided more focused evidence. In this study, FA showed extensive involvement of tracts in comprehension

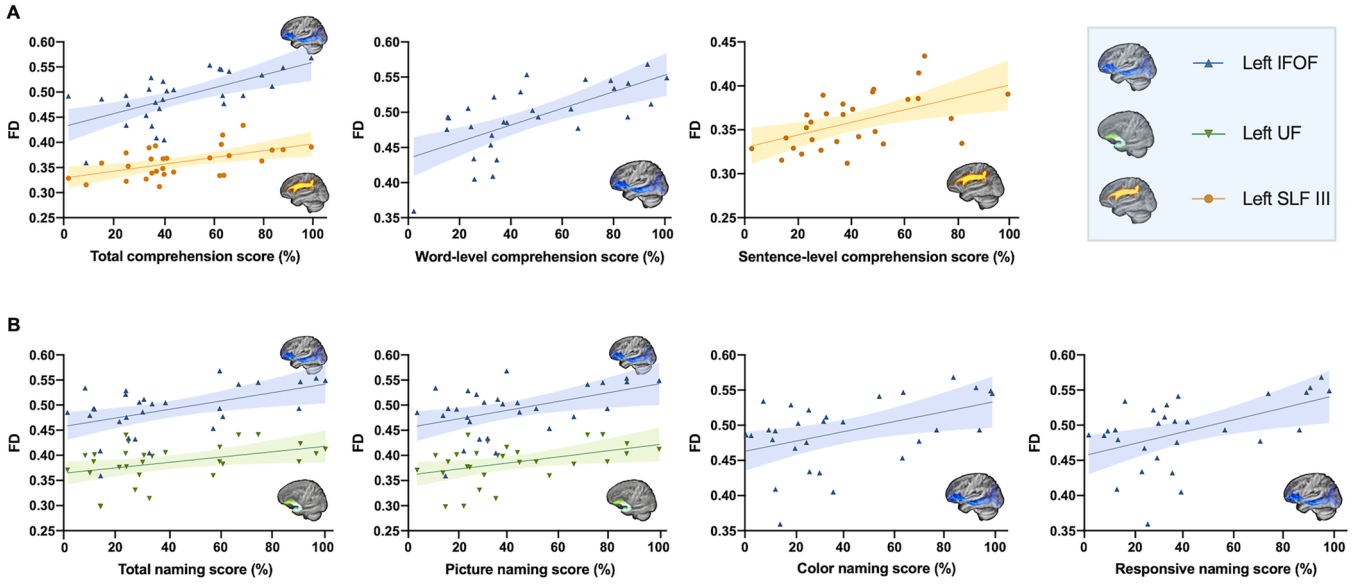

Fig. 7. Significant correlations between language scores and tract-wise fiber density (FD) in post-stroke aphasia (Bonferroni corrected $p < 0.05$). A, The scatter plots depict the correlations with the comprehension domain. B, The scatter plots depict the correlations with the naming domain.

processing, while fixel-wise FD correlations with comprehension focused on the IFOF. In addition, FBA emphasizes the precise language-tract mapping at a more subdivided level of the IFOF, and reveals dissociable correlations with language subdomains.

The linguistic role of the left UF has been debated for decades despite increasing evidence supporting its semantic associations (Han et al., 2013; Harvey et al., 2013; Marchina et al., 2011; Xing et al., 2017; Zhang et al., 2018). The linguistic role of the left UF was once regarded as being misguided by the indistinct delineation of *in vivo* tractography of overlapping tracts, given that it was sometimes difficult to separate the IFOF from the UF during post-mortem dissection (Peltier et al., 2010). With the help of the fiber-specific tool, our study disentangled the crossing fibers and yielded more convincing evidence for the controversial language mapping. The UF-naming association revealed by our FBA method is in accordance with the high-grade evidence obtained from surgical removal and electrostimulation mapping (Papagno et al., 2011). In addition, a recent diffusion spectrum imaging study also indicates that the UF played a critical role in semantic processing for word production (Hula et al., 2020).

4.4. Strengths and limitations

To the best of our knowledge, this is the first study to use a fiber-specific tool for examining dual-stream pathways in post-stroke aphasic patients. The strengths of this study include use of an advanced diffusion model (CSD) to detect crossing-fiber populations of dual-stream pathways. FBA-VBA mismatch interprets the underlying configuration of specific crossing fibers. Compared with FA, FBA findings provide more accurate localization and microstructural pathology for language pathways. Tract-wise fixel metrics depict the characteristics of average statistics along the whole course of a specific tract and reveal dissociable subdomain correlations. Despite above promising advantages, the present study was limited by the heterogeneity of the symptoms of aphasia profiles. The relatively small sample size reduced statistical power and precluded the investigation of subgroup differences. Template-based tractography may lead to insufficient capture of inter-individual variability in tract morphology for the patients with stroke. In addition, the quality of DWI data need to be improved considering the diffusion direction number of this study were small. Finally, this study did not include follow-up evaluations at the chronic stage, and longitudinal changes were not addressed.

4.5. Future directions

A larger cohort would be useful to facilitate the understanding of the fiber-specific associations of patients with different aphasic subtypes. Follow-up studies are needed to detect the value of fixel-based morphometry in predicting longitudinal behavioral changes. Furthermore, FBA might be a promising technique in mapping fiber-specific white matter pathologies related to other post-stroke neurological deficits, such as sensory and cognitive impairment.

5. Conclusions

This study demonstrates fixel-based analysis in patients with post-stroke aphasia can identify fiber-specific damage of dual streams in crossing-fiber regions and indicates improved ability of fixel-based metrics compared to conventional DTI metrics in language network research. Fiber density reductions of dual streams suggest that fiber-specific intra-axonal volume reduction is the microstructural damage of white matter integrity. Fixel-based language mapping exhibits more precise location than voxel-wise DTI metrics, mapping comprehension associations at subdivided segments of the left IFOF. It also yields fiber-specific evidence for the debated association between the left UF and naming disability. Additionally, fixel-based language mapping reveals dissociative associations, attributing different language subdomains to distinct tracts.

CRediT authorship contribution statement

Conceptualization: Benyan Luo; Methodology: Dan Wu and Weihao Zheng; Investigation: Desheng Shang, Lingling Li, Jing Ye, and Yamei Yu; Formal analysis: Weihao Zheng, Shuchang Zhong and Jie Zhang; Funding acquisition: Benyan Luo and Jie Zhang; Figure: Li Zhang and Ruidong Cheng; Writing - original draft: Jie Zhang; Revision: Yating Chen and Jie Zhang; Writing - review & editing: Xiangming Ye and Fangping He; Supervision: Benyan Luo.

Declaration of Competing Interest

The authors declare that they have no known competing financial interests or personal relationships that could have appeared to influence the work reported in this paper.

Acknowledgments

This study was funded by grants from the National Natural Science Foundation of China (81902278 and 81870817).

Appendix A. Supplementary data

Supplementary data to this article can be found online at https://doi.org/10.1016/j.nicl.2021.102774.

References

Andersson, J.L.R., Graham, M.S., Drobnjak, I., Zhang, H., Filippini, N., Bastiani, M., 2017. Towards a comprehensive framework for movement and distortion correction of diffusion MR images: Within volume movement. Neuroimage. 152, 450–466. https://doi.org/10.1016/j.neuroimage.2017.02.085.

Andersson, J.L.R., Graham, M.S., Zsoldos, E., Sotiropoulos, S.N., 2016. Incorporating outlier detection and replacement into a non-parametric framework for movement and distortion correction of diffusion MR images. Neuroimage. 141, 556–572. https://doi.org/10.1016/j.neuroimage.2016.06.058.

Andersson, J.L.R., Sotiropoulos, S.N., 2016. An integrated approach to correction for off-resonance effects and subject movement in diffusion MR imaging. Neuroimage. 125, 1063–1078. https://doi.org/10.1016/j.neuroimage.2015.10.019.

Avants, B.B., Tustison, N.J., Song, G., Cook, P.A., Klein, A., Gee, J.C., 2011. A reproducible evaluation of ANTs similarity metric performance in brain image registration. Neuroimage. 54 (3), 2033–2044. https://doi.org/10.1016/j.neuroimage.2010.09.025.

Bernhardt, J., Hayward, K.S., Kwakkel, G., Ward, N.S., Wolf, S.L., Borschmann, K., Krakauer, J.W., Boyd, L.A., Carmichael, S.T., Corbett, D., Cramer, S.C., 2017. Agreed Definitions and a Shared Vision for New Standards in Stroke Recovery Research: The Stroke Recovery and Rehabilitation Roundtable Taskforce. Neurorehabil Neural Repair. 31 (9), 793–799. https://doi.org/10.1177/1545968317732668.

Berthier, M.L., 2005. Poststroke aphasia : epidemiology, pathophysiology and treatment. Drugs Aging. 22 (2), 163–182. https://doi.org/10.2165/00002512-200522020-00006.

Carotenuto, A., Cocozza, S., Quarantelli, M., Arcara, G., Lanzillo, R., Brescia Morra, V., Cerillo, I., Tedeschi, E., Orefice, G., Bambini, V., Brunetti, A., Iodice, R., 2018. Pragmatic abilities in multiple sclerosis: The contribution of the temporo-parietal junction. Brain Lang. 185, 47–53. https://doi.org/10.1016/j.bandl.2018.08.003.

Carter, R.M., Huettel, S.A., 2013. A nexus model of the temporal-parietal junction. Trends Cogn Sci. 17 (7), 328–336. https://doi.org/10.1016/j.tics.2013.05.007.

Catani, M., Howard, R.J., Pajevic, S., Jones, D.K., 2002. Virtual in vivo interactive dissection of white matter fasciculi in the human brain. Neuroimage. 17 (1), 77–94. https://doi.org/10.1006/nimg.2002.1136.

Catani, M., Mesulam, M. M., Jakobsen, E., Malik, F., Martersteck, A., Wieneke, C., et al., 2013. A novel frontal pathway underlies verbal fluency in primary progressive aphasia. Brain. 136 (Pt 8), 2619-2628. https://doi.org/10.1093/brain/awt163.

Corbetta, M., Ramsey, L., Callejas, A., Baldassarre, A., Hacker, C., Siegel, J., Astafiev, S., Rengachary, J., Zinn, K., Lang, C., Connor, L., Fucetola, R., Strube, M., Carter, A., Shulman, G., 2015. Common behavioral clusters and subcortical anatomy in stroke. Neuron. 85 (5), 927–941. https://doi.org/10.1016/j.neuron.2015.02.027.

Crinion, J., Price, C.J., 2005. Right anterior superior temporal activation predicts auditory sentence comprehension following aphasic stroke. Brain. 128 (Pt 12), 2858–2871. https://doi.org/10.1093/brain/awh659.

Duffau, H., Herbet, G., Moritz-Gasser, S., 2013. Toward a pluri-component, multimodal, and dynamic organization of the ventral semantic stream in humans: lessons from stimulation mapping in awake patients. Front. Syst. Neurosci. 7, 44. https://doi.org/10.3389/fnsys.2013.00044.

Egorova, N., Dhollander, T., Khlif, M.S., Khan, W., Werden, E., Brodtmann, A., 2020. Pervasive White Matter Fiber Degeneration in Ischemic Stroke. Stroke. 51 (5), 1507–1513. https://doi.org/10.1161/STROKEAHA.119.028143.

Forkel, S. J., De Schotten, M. T., Dell'Acqua, F., Kalra, L., Murphy, D. G. M., Williams, S. C. R., et al., 2014. Anatomical predictors of aphasia recovery: A tractography study of bilateral perisylvian language networks. Brain. 137 (7), 2027-2039. https://doi.org/10.1093/brain/awu113.

Forkel, S.J., Rogalski, E., Drossinos Sancho, N., D'Anna, L., Luque Laguna, P., Sridhar, J., Dell'Acqua, F., Weintraub, S., Thompson, C., Mesulam, M.-M., Catani, M., 2020. Anatomical evidence of an indirect pathway for word repetition. Neurology. 94 (6), e594–e606. https://doi.org/10.1212/WNL.0000000000008746.

Fridriksson, J., Kjartansson, O., Morgan, P.S., Hjaltason, H., Magnusdottir, S., Bonilha, L., Rorden, C., 2010. Impaired speech repetition and left parietal lobe damage. J Neurosci. 30 (33), 11057–11061. https://doi.org/10.1523/JNEUROSCI.1120-10.2010.

Friederici, A.D., 2012. The cortical language circuit: from auditory perception to sentence comprehension. Trends Cogn Sci. 16 (5), 262–268. https://doi.org/10.1016/j.tics.2012.04.001.

Gao, S.R., 2006. Aphasia, Second Edition. Peking University Medical Press, Beijing, China.

Grazioplene, R.G., Bearden, C.E., Subotnik, K.L., Ventura, J., Haut, K., Nuechterlein, K. H., Cannon, T.D., 2018. Connectivity-enhanced diffusion analysis reveals white matter density disruptions in first episode and chronic schizophrenia. Neuroimage Clin. 18, 608–616. https://doi.org/10.1016/j.nicl.2018.02.015.

Greve, D.N., Fischl, B., 2009. Accurate and robust brain image alignment using boundary-based registration. Neuroimage. 48 (1), 63–72. https://doi.org/10.1016/j.neuroimage.2009.06.060.

Han, Z., Ma, Y., Gong, G., He, Y., Caramazza, A., Bi, Y., 2013. White matter structural connectivity underlying semantic processing: evidence from brain damaged patients. Brain. 136, 2952–2965. https://doi.org/10.1093/brain/awt205.

Han, Z., Ma, Y., Gong, G., Huang, R., Song, L., Bi, Y., 2016. White matter pathway supporting phonological encoding in speech production: a multi-modal imaging study of brain damage patients. Brain Struct Funct. 221 (1), 577–589. https://doi.org/10.1007/s00429-014-0926-2.

Harvey, D.Y., Schnur, T.T., 2015. Distinct loci of lexical and semantic access deficits in aphasia: Evidence from voxel-based lesion-symptom mapping and diffusion tensor imaging. Cortex. 67, 37–58. https://doi.org/10.1016/j.cortex.2015.03.004.

Harvey, D.Y., Wei, T., Ellmore, T.M., Hamilton, A.C., Schnur, T.T., 2013. Neuropsychological evidence for the functional role of the uncinate fasciculus in semantic control. Neuropsychologia. 51 (5), 789–801. https://doi.org/10.1016/j.neuropsychologia.2013.01.028.

Hau, J., Sarubbo, S., Houde, J.C., Corsini, F., Girard, G., Deledalle, C., Crivello, F., Zago, L., Mellet, E., Jobard, G., Joliot, M., Mazoyer, B., Tzourio-Mazoyer, N., Descoteaux, M., Petit, L., 2017. Revisiting the human uncinate fasciculus, its subcomponents and asymmetries with stem-based tractography and microdissection validation. Brain Struct Funct. 222 (4), 1645–1662. https://doi.org/10.1007/s00429-016-1298-6.

Hickok, G., Poeppel, D., 2007. The cortical organization of speech processing. Nat Rev Neurosci. 8 (5), 393–402. https://doi.org/10.1038/nrn2113.

Hula, W. D., Panesar, S., Gravier, M. L., Yeh, F. C., Dresang, H. C., Dickey, M. W., et al., 2020. Structural white matter connectometry of word production in aphasia: an observational study. Brain. 143 (8), 2532-2544. https://doi.org/10.1093/brain/awaa193.

Ivanova, M.V., Isaev, D.Y., Dragoy, O.V., Akinina, Y.S., Petrushevskiy, A.G., Fedina, O.N., Shklovsky, V.M., Dronkers, N.F., 2016. Diffusion-tensor imaging of major white matter tracts and their role in language processing in aphasia. Cortex. 85, 165–181. https://doi.org/10.1016/j.cortex.2016.04.019.

Jeurissen, B., Leemans, A., Tournier, J.D., Jones, D.K., Sijbers, J., 2013. Investigating the prevalence of complex fiber configurations in white matter tissue with diffusion magnetic resonance imaging. Hum Brain Mapp. 34 (11), 2747–2766. https://doi.org/10.1002/hbm.22099.

Johansenberg, H.B.T., Behrens, T.E.J., 2013. Diffusion MRI: From Quantitative Measurement to In vivo Neuroanatomy, 2nd. Elsevier.

Kim, S.H., Jang, S.H., 2013. Prediction of aphasia outcome using diffusion tensor tractography for arcuate fasciculus in stroke. AJNR Am. J. Neuroradiol. 34 (4), 785–790. https://doi.org/10.3174/ajnr.A3259.

Kyeong, S., Kang, H., Kyeong, S., Kim, D.H., 2019. Differences in Brain Areas Affecting Language Function After Stroke. Stroke. 50 (10), 2956–2959. https://doi.org/10.1161/STROKEAHA.119.026222.

Marchina, S., Zhu, L.L., Norton, A., Zipse, L., Wan, C.Y., Schlaug, G., 2011. Impairment of speech production predicted by lesion load of the left arcuate fasciculus. Stroke. 42 (8), 2251–2256. https://doi.org/10.1161/strokeaha.110.606103.

Marin, M.A., Carmichael, S.T., 2019. Mechanisms of demyelination and remyelination in the young and aged brain following white matter stroke. Neurobiol Dis. 126, 5–12. https://doi.org/10.1016/j.nbd.2018.07.023.

Mito, R., Raffelt, D., Dhollander, T., Vaughan, D. N., Tournier, J. D., Salvado, O., et al., 2018. Fibre-specific white matter reductions in Alzheimer's disease and mild cognitive impairment. Brain. 141 (3), 888-902. https://doi.org/10.1093/brain/awx355.

Pani, E., Zheng, X., Wang, J., Norton, A., Schlaug, G., 2016. Right hemisphere structures predict poststroke speech fluency. Neurology. 86 (17), 1574–1581. https://doi.org/10.1212/wnl.0000000000002613.

Pannek, K., Fripp, J., George, J.M., Fiori, S., Colditz, P.B., Boyd, R.N., Rose, S.E., 2018. Fixel-based analysis reveals alterations in brain microstructure and macrostructure of preterm-born infants at term equivalent age. Neuroimage Clin. 18, 51–59. https://doi.org/10.1016/j.nicl.2018.01.003.

Papagno, C., Miracapillo, C., Casarotti, A., Romero Lauro, L.J., Castellano, A., Falini, A., Casaceli, G., Fava, E., Bello, L., 2011. What is the role of the uncinate fasciculus? Surgical removal and proper name retrieval. Brain. 134 (2), 405–414. https://doi.org/10.1093/brain/awq283.

Pecheva, D., Tournier, J.-D., Pietsch, M., Christiaens, D., Batalle, D., Alexander, D.C., Hajnal, J.V., Edwards, A.D., Zhang, H., Counsell, S.J., 2019. Fixel-based analysis of the preterm brain: Disentangling bundle-specific white matter microstructural and macrostructural changes in relation to clinical risk factors. Neuroimage Clin. 23, 101820. https://doi.org/10.1016/j.nicl.2019.101820.

Peltier, J., Verclytte, S., Delmaire, C., Pruvo, J.P., Godefroy, O., Le Gars, D., 2010. Microsurgical anatomy of the temporal stem: clinical relevance and correlations with diffusion tensor imaging fiber tracking. J Neurosurg. 112 (5), 1033–1038. https://doi.org/10.3171/2009.6.JNS08132.

Raffelt, D.A., Smith, R.E., Ridgway, G.R., Tournier, J.-D., Vaughan, D.N., Rose, S., Henderson, R., Connelly, A., 2015. Connectivity-based fixel enhancement: Whole-brain statistical analysis of diffusion MRI measures in the presence of crossing fibres. Neuroimage. 117, 40–55. https://doi.org/10.1016/j.neuroimage.2015.05.039.

Raffelt, D.A., Tournier, J.-D., Smith, R.E., Vaughan, D.N., Jackson, G., Ridgway, G.R., Connelly, A., 2017. Investigating white matter fibre density and morphology using fixel-based analysis. Neuroimage. 144, 58–73. https://doi.org/10.1016/j.neuroimage.2016.09.029.

Rau, Y.-A., Wang, S.-M., Tournier, J.-D., Lin, S.-H., Lu, C.-S., Weng, Y.-H., Chen, Y.-L., Ng, S.-H., Yu, S.-W., Wu, Y.-M., Tsai, C.-C., Wang, J.-J., 2019. A longitudinal fixel-based analysis of white matter alterations in patients with Parkinson's disease. Neuroimage Clin. 24, 102098. https://doi.org/10.1016/j.nicl.2019.102098.

Riffert, T.W., Schreiber, J., Anwander, A., Knosche, T.R., 2014. Beyond fractional anisotropy: extraction of bundle-specific structural metrics from crossing fiber models. Neuroimage. 100, 176–191. https://doi.org/10.1016/j.neuroimage.2014.06.015.

Saur, D., Kreher, B.W., Schnell, S., Kümmerer, D., Kellmeyer, P., Vry, M.-S., Umarova, R., Musso, M., Glauche, V., Abel, S., Huber, W., Rijntjes, M., Hennig, J., Weiller, C., 2008. Ventral and dorsal pathways for language. Proc Natl Acad Sci U S A. 105 (46), 18035–18040. https://doi.org/10.1073/pnas.0805234105.

Smith, R.E., Tournier, J.D., Calamante, F., Connelly, A., 2013. SIFT: Spherical-deconvolution informed filtering of tractograms. Neuroimage. 67, 298–312. https://doi.org/10.1016/j.neuroimage.2012.11.049.

Tournier, J.D., Calamante, F., Connelly, A., 2007. Robust determination of the fibre orientation distribution in diffusion MRI: non-negativity constrained super-resolved spherical deconvolution. Neuroimage. 35 (4), 1459–1472. https://doi.org/10.1016/j.neuroimage.2007.02.016.

Tournier, J.-D., Smith, R., Raffelt, D., Tabbara, R., Dhollander, T., Pietsch, M., Christiaens, D., Jeurissen, B., Yeh, C.-H., Connelly, A., 2019. MRtrix3: A fast, flexible and open software framework for medical image processing and visualisation. Neuroimage. 202, 116137. https://doi.org/10.1016/j.neuroimage.2019.116137.

Verhelst, H., Giraldo, D., Vander Linden, C., Vingerhoets, G., Jeurissen, B., Caeyenberghs, K., 2019. Cognitive Training in Young Patients With Traumatic Brain Injury: A Fixel-Based Analysis. Neurorehabil Neural Repair. 33 (10), 813–824. https://doi.org/10.1177/1545968319868720.

Wallace, E.J., Mathias, J.L., Ward, L., Fripp, J., Rose, S., Pannek, K., 2020. A fixel-based analysis of micro- and macro-structural changes to white matter following adult traumatic brain injury. Hum Brain Mapp. 41 (8), 2187–2197. https://doi.org/10.1002/hbm.v41.810.1002/hbm.24939.

Warrington, S., Bryant, K.L., Khrapitchev, A.A., Sallet, J., Charquero-Ballester, M., Douaud, G., Jbabdi, S., Mars, R.B., Sotiropoulos, S.N., 2020. XTRACT - Standardised protocols for automated tractography in the human and macaque brain. Neuroimage. 217, 116923. https://doi.org/10.1016/j.neuroimage.2020.116923.

Xing, S., Lacey, E.H., Skipper-Kallal, L.M., Zeng, J., Turkeltaub, P.E., 2017. White Matter Correlates of Auditory Comprehension Outcomes in Chronic Post-Stroke Aphasia. Front Neurol. 8, 54. https://doi.org/10.3389/fneur.2017.00054.

Yang, M., Li, Y., Li, J., Yao, D., Liao, W., Chen, H., 2017. Beyond the Arcuate Fasciculus: Damage to Ventral and Dorsal Language Pathways in Aphasia. Brain Topogr. 30 (2), 249–256. https://doi.org/10.1007/s10548-016-0503-5.

Zarkali, A., McColgan, P., Leyland, L.A., Lees, A.J., Rees, G., Weil, R.S., 2020. Fiber-specific white matter reductions in Parkinson hallucinations and visual dysfunction. Neurology. 94 (14), e1525–e1538. https://doi.org/10.1212/WNL.0000000000009014.

Zhang, J., Wei, X., Xie, S., Zhou, Z., Shang, D., Ji, R., Yu, Y., He, F., Du, Y., Ye, X., Luo, B., 2018. Multifunctional Roles of the Ventral Stream in Language Models: Advanced Segmental Quantification in Post-Stroke Aphasic Patients. Front Neurol. 9 https://doi.org/10.3389/fneur.2018.0008910.3389/fneur.2018.00089.s001.

Zhang, J., Zhong, S., Zhou, L., Yu, Y., Tan, X., Wu, M., et al., 2021. Correlations between Dual-Pathway White Matter Alterations and Language Impairment in Patients with Aphasia: A Systematic Review and Meta-analysis. Neuropsychol Rev. 1-17. https://doi.org/10.1007/s11065-021-09482-8.

Zhang, Y., Wang, C., Zhao, X., Chen, H., Han, Z., Wang, Y., 2010. Diffusion tensor imaging depicting damage to the arcuate fasciculus in patients with conduction aphasia: a study of the Wernicke-Geschwind model. Neurol Res. 32 (7), 775–778. https://doi.org/10.1179/016164109x12478302362653.